J Korean Med Sci 2001; 16: 294-302
ISSN 1011-8934

Viable Myocardium in Reperfused Acute Myocardial Infarction: Rest and Stress First-Pass MR Imaging

Feasibility of identifying viable myocardium in rest and stress magnetic resonance imaging (MRI) was evaluated using 3 hr occlusion and 30 min reperfusion model of left anterior descending (LAD) coronary artery in 12 felines. At rest MRI, viable myocardium confirmed by 2,3,5-triphenyl tetrazolium chloride (TTC)-staining showed rapid signal intensity (SI) rise followed by gradual decline not significantly different from normal myocardium that the two hyperperfused regions were distinguishable only from the hypoperfused nonviable myocardium. At stress MRI, hyperemia induced perfusion change was most pronounced in normal myocardium with earlier and greater peak enhancement followed by brisk 'washout' phase while minimally augmented enhancement in viable myocardium was still in 'washin' phase. From these findings, it was concluded that viable myocardium is identified in rest and stress MRI as redistributing hypo-perfusion compared to persistent hyper-perfusion of the normal myocardium and the persistent hypo-perfusion of the nonviable myocardium.

Key Words : *Perfusion Heart; Magnetic Resonance Spectroscopy; Myocardial Infarction; Myocardium; Myocardial Reperfusion; Image Enhancement*

Kyung Il Chung, Tae-Sub Chung*, Richard D. White†, Hanns-J. Weinmann†, Tae-Hwan Lim§, Byung-Il Choi||, Jung-Ho Suh

Departments of Radiology, Cardiology||, Ajou University School of Medicine, Suwon, Korea; Department of Radiology*, Yonsei University Medical College, Seoul, Korea; Division of Radiology†, The Cleveland Clinic Foundation, Cleveland, OH, U.S.A.; Schering AG†, Diagnostic Imaging Division, Contrast Media Research, Berlin, Germany; Department of Radiology§, University of Ulsan College of Medicine, Seoul, Korea

Received : 14 August 2000
Accepted : 1 February 2001

Address for correspondence
Kyung Il Chung, M.D.
Department of Diagnostic Radiology, Ajou University Hospital, San 5, Wonchon-dong, Paldal-gu, Suwon 442-749, Korea
Tel : +82.31-219-5857, Fax : +82.31-219-5862
E-mail : chki@madang.ajou.ac.kr

• This study was partially contributed by funds from GE medical systems and Schering AG.

INTRODUCTION

Viable myocardium has great significance in the treatment of acute myocardial infarction as prompt reperfusion before the onset of irreversible damage may salvage the viable myocardium greatly improving the patient outcome. The success of such therapy is dependent on the extent of the reperfusion accomplished and determination of such success necessitates documentation of the extent of reperfusion and identification of reversible from the irreversible injury (1, 2).

Commonly established clinical methods for assessing myocardial viability include thallium imaging and echocardiography (2, 3). Recently, much emphasis has been on MRI for its dual capabilities of qualitative and quantitative analysis as the recent fast MR imaging enables not only the morphologic depiction but also the function and the precise characterization of regional perfusion.

Various previous efforts demonstrated the potential of MR imaging for discriminating occlusive and reperfused infarctions and for differentiating reperfused reversible and irreversible myocardial injuries (1). However, the role of MRI in providing information regarding the viability within the injury zone is still uncertain. With the first-pass MRI already well established as an accurate mean of accessing myocardial perfusion (4), we performed this study to determine the feasibility of stress and rest MRI in identifying viable myocardium from the more severe myocardial injuries and to characterize the perfusion kinetics.

MATERIALS AND METHODS

Animal preparation

Twelve adult felines weighing 3,100-4,200 g (mean; 3,780 g) were examined. Atropine sulfate (0.05 mg/kg) was pre-administered intramuscularly and the animals were sedated with ketamin (10 mg/kg). After intubation, each cat was anesthetized with 5% halothane administered using a mechanical ventilator (R-60; Aika Medical

Corp., Matsudo City, Japan). Both femoral veins were cannulated for separate administration of drugs and contrast media. Pancuronium bromide (0.6 mg/kg) was used for skeletal muscle relaxation.

Left lateral thoracotomy was performed followed by midline incision of the pericardium. Left anterior descending (LAD) coronary artery was exposed and ligated distal to the first diagonal with 4-0 silk. LAD artery occlusion was confirmed by cyanosis of the myocardium at risk and was maintained for 3 hr. Following the removal of the silk ligature, reperfusion was confirmed by the return of the normal myocardial complexion and was maintained for 30 min.

Stress (hyperemic) agent

We used adenosine 5'-triphosphate (ATP) as a stress agent to achieve hyperemic response within the myocardium. ATP is known to have vasodilator potency and fewer hemodynamic or electrocardiographic derangements compared to papaverine (5, 6) and reports also showed that ATP has greater vasodilator potency than adenosine and dipyridamole (7-9).

MR imaging

MR images were acquired on a 1.5-T unit (Signa, General Electric Medical systems, Milwaukee, WI, U.S.A.) using extremity coil. Baseline transaxial imaging was undertaken using spin-echo (SE) and fast gradient-recalled echo (FGRE) sequences. The third slice location from the apex was selected for the first-pass imaging.

At the commencement of the 30 min reperfusion period, ATP (0.14 mg/kg/min) was infused for 6 min through the left femoral vein using an injection pump. At the third minute of the infusion, a bolus (0.1 mmol Gd/kg) of Gadomer-17 (Schering AG, Berlin, Germany) was administered through the contra-lateral femoral vein and first-pass imaging was initiated using FGRE sequence with following parameters: TR/TE=9.4/2.2, slice thickness=5 mm, matrix size=256×128, field of view=120 mm, flip angle=30°, bandwidth=15 kHz. Using sequential acquisition order, 60 consecutive images were obtained every 1.24 sec without any interscan delays.

Equilibrium state SE imaging was performed using following parameters: TR=~400 (variable with heart rate), TE=15, slice thickness=5 mm, matrix=256×128, field of view=120 mm, number of excitation=2. Images were obtained at 5, 10, 15, 30, 45, and 60 min after the contrast administration.

Subsequent interval of 1 hr allowed a total of 2 hr (including the equilibrium state imaging time) for adequate elimination of contrast media from the myocardium. Aforementioned imaging protocol was then repeated for the resting state imaging.

Postmortem histochemical staining

Upon the completion of the imaging protocol, the animals were sacrificed by injecting a lethal dose of potassium chloride solution. After cardiectomy, the aorta and LAD artery were cannulated and respective methylene blue (20 mL) and TTC (10 mL) solutions were infused to allow myocardial staining. After storage in 10% formalin solution for 12 hr, each heart was excised in the same plane as in MR imaging.

Image analysis

Viability categorization was according to the following in SE imaging with confirmation by specimen stain; 1) normal myocardium with moderate enhancement in posterolateral wall, 2) viable myocardium in hyper-enhancing peri-infarct zone in subepicardial anterior wall, and 3) nonviable myocardium in infarct core in subendocardial anterior wall. Corresponding areas of myocardium were analyzed on first-pass images for the possibility of identifying the viable myocardium. The myocardial SI within a region of interest (ROI) of 0.25-0.5 cm^2 was measured on a workstation (Sparc, Sun Microsystems, Mountain View, CA, U.S.A.) and normalized relative to the values of the posterior chestwall musculature.

The normalized data was linearly interpolated to plot the SI at each second for the first minute of the first-pass transit. From the first-pass profile consisting of bolus 'washin' (upslope) and 'washout' (downslope) phases, minimum and maximum SI (SI_{min}, SI_{max}) achieved during the 'washin' phase and their respective time points (T_{min}, T_{max}) were recorded. The slope of the 'washin' phase was estimated using linear regression method.

The ratio of maximum SI (SI_{max} Ratio) and maximum of SI difference (Max ΔSI) between ischemic (viable or nonviable) and normal myocardium were measured. The above perfusion parameters were averaged among the 12 cases to estimate the final value which was described as mean±standard error. The results acquired during both stress and rest were then evaluated for the possibility of providing the information regarding the status of the myocardial viability.

The paired two-tailed Student's t-test was used to determine significant alteration in SI from the baseline following administration of MR contrast media and to evaluate the effect of pharmacologic stress on the alteration of the SI. The one way analysis of variance (ANOVA) with multiple comparison of the mean values using Scheffe's F-test was used to determine the signifi-

cant differences of SI alteration over time among the myocardial zones. The peak SI and the slope of initial SI rise were also analyzed using both the paired t-test and ANOVA. In all cases, statistical significance was defined as $p<0.05$.

RESULTS

Myocardial perfusion in rest (basal) state

After the administration of Gadomer-17, initial short drop from baseline SI to minimum SI (SI_{min}) was followed by upsurge in myocardial enhancement (Fig. 1A). The drop to SI_{min} was most significant in nonviable myocardium occurring later than other myocardial zones (Table 1, 2).

The enhancement in normal and viable myocardium upsurged to the maximum SI (SI_{max}) of 1.627 ± 0.044 and 1.430 ± 0.044, respectively, while the enhancement in nonviable myocardium was insignificant.

Normal myocardium showed most rapid slope not significantly different from the viable myocardium. Nonviable myocardium showed gradual slope significantly

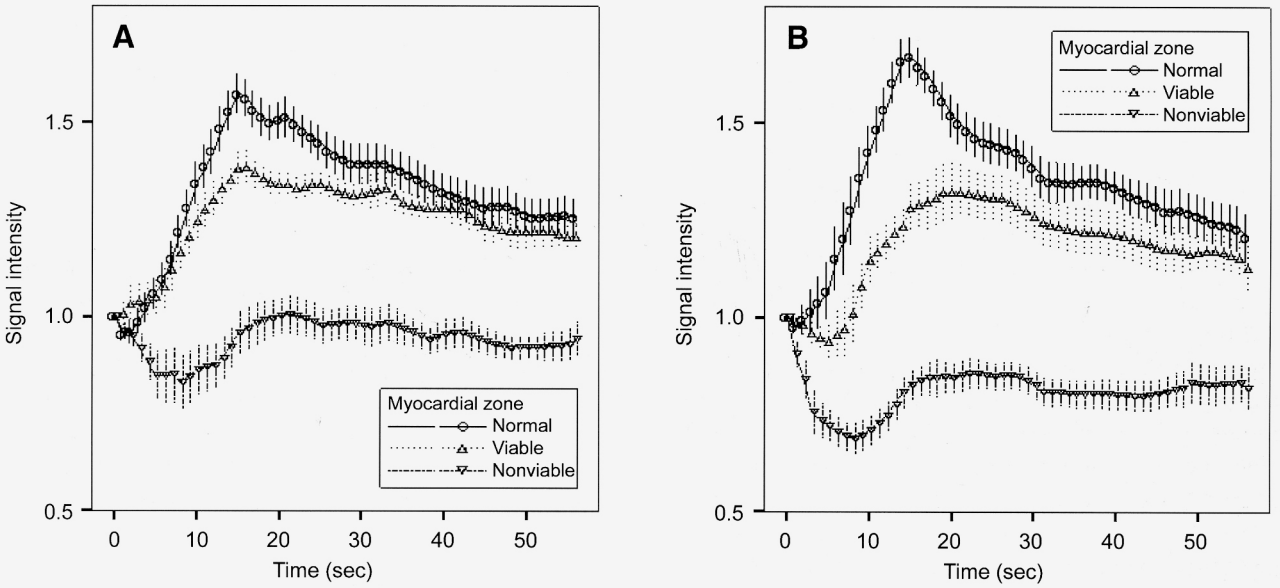

Fig. 1. Signal intensity (SI)-time curves from 3 hr occlusion and 30 min reperfusion models of cat myocardium during resting-state (A) and stressed-state (B) first-pass transit of Gadomer-17. Dispersion of bolus profiles especially between normal myocardium and reversibly injured viable myocardium is evident during stress (B) particularly at the earlier portion of the curves leading to the identification of the viable myocardium as in Fig. 2.

Table 1. Perfusion parameters of myocardial zones (normal, viable, nonviable) in rest and stress MRI†

Perfusion parameters	Normal		Viable		Nonviable		r‡	
	Rest	Stress	Rest	Stress	Rest	Stress	Rest	Stress
T_{min}	1±0	1±1	2±1	4±1	6±1	6±1	.534	.607
T_{max}	16±1	14±1	19±2	18±1	21±2	21±1	.342	.575
SI_{min}	.929±.021*	.910±.047	.927±.025*	.817±.054*	.735±.058*	.610±.044*	.522	.614
SI_{max}	1.627±.044*	1.724±.048*	1.430±.044*	1.378±.063*	1.071±.052	.912±.037*	.827	.898
Slope	.049±.004	.068±.005	.033±.006	.044±.005	.022±.005	.020±.002	.571	.817
SI_{max} ratio			.888±.026	.802±.031	.666±.033	.542±.028	.842	.927
Max ⊿SI			.233±.062	.515±.039	.676±.078	.910±.065	.830	.937

T_{min}, time to minimum signal intensity (SI) in seconds; T_{max}, time to maximum SI in seconds; SI_{min}, minimum SI; SI_{max}, maximum SI; SI_{max} ratio, ratio of maximum SI between ischemic (viable or nonviable) and normal myocardium; Max ⊿SI, maximum of SI difference between ischemic (viable or nonviable) and normal myocardium

*Significantly ($p<0.05$) different from baseline preinjection values.

†Values are mean±standard error of the mean.

‡Correlation coefficients for myocardial viability (normal, viable, nonviable) versus perfusion parameters.

Table 2. comparison of perfusion parameters among myocardial zones (Scheffe's F-test) and between rest and stress state (paired two-tailed Student's t-test)†

Perfusion parameters	Scheffe's F-test						Paired two-tailed Student's t-test		
	Normal vs viable		Normal vs nonviable		Viable vs nonviable				
	Rest	Stress	Rest	Stress	Rest	Stress	Normal	Viable	Nonviable
T_{min}	.874	.148	.004	.001	.015	.108	.992	.155	.698
T_{max}	.610	.093	.145	.002	.610	.288	.038	.761	.771
SI_{min}	.999	.402	.004	.001	.005	.020	.609	.068	.007
SI_{max}	.019	.000	.000	.000	.000	.000	.002	.533	.002
Slope	.100	.001	.002	.000	.287	.003	.008	.190	.791
SI_{max} ratio					.000	.000		.107	.001
Max ΔSI					.000	.000		.004	.016

†Abbreviations as in Table 1. Figures represent *p* values

different only from the normal myocardium (Table 2).

Maximum of SI difference (Max ΔSI) between ischemic (viable or nonviable) and normal myocardium was attained at 15 sec post-contrast, not significantly different from the time of the maximum SI (T_{max}) for the normal myocardium. The SI difference between viable and normal myocardium was relatively small consistent with the proximity of the bolus transits maintained by the viable and normal myocardium (Table 1) and therefore, the two myocardial zones were not distinguishable in FGRE imaging (Fig. 2A). However, adequate SI difference led to fine depiction of the hypo-perfused nonviable myocardium from the surrounding hyper-perfused viable and normal myocardium.

Myocardial perfusion in stress (hyperemic) state

At stress, enhancement of the normal myocardium upsurged to the significantly higher SI_{max} of 1.724 ± 0.048 than at rest followed by more brisk return toward the baseline SI (Table 1, 2, Fig. 1B). Enhancement of the viable myocardium remained not significantly different from that at rest reaching the SI_{max} of 1.378 ± 0.063 while the SI_{max} of the nonviable myocardium was significantly below the baseline level. T_{max} in normal myocardium was significantly earlier than that at resting state leading to more apparent time difference from the viable myocardium and significant difference from the nonviable myocardium (Table 2).

Normal myocardium showed significantly more rapid slope than at resting state while viable myocardium showed insignificant augmentation of the moderate slope and nonviable myocardium showed persistent gradual slope. These responses led to significantly different rates of the SI rise among the myocardial zones (Table 2).

Max ΔSI between ischemic and normal myocardium was much greater occurring at an earlier post-contrast time of 13 sec which approximated T_{max} of the normal myocardium. There was no significant difference in the time of Max ΔSI between viable and nonviable myocardium.

Postmortem findings

The redistributed hypo-perfusion in first-pass imaging, which corresponded to the outer peri-infarct zone in equilibrium state SE imaging, was in agreement with the brick-red colored TTC-positive area as the reversible viable myocardium. The persistent hypo-perfusion in first-pass imaging, which corresponded to the infarct center in equilibrium state SE imaging, was corroborated by TTC-negative irreversible nonviable myocardium (Fig. 2).

DISCUSSION

In reperfused infarction, the territory composed primarily of irreversibly injured myocardium undergoes myocyte perishment followed by damage to the microvascular endothelium leading to leakage of macromolecules and the consequent tissue swelling resulting in reduced blood volume and perfusion (10, 11). At the very core of the infarction, however, myocytes may undergo simultaneous necrosis with the capillaries which become occluded by dying cells and debris; the infarct core may, therefore, be unresponsive to restoration of epicardial blood flow (1, 10, 12). These changes, on the other hand, are minimal in reversibly injured myocardium bordering the infarction where the recovery of cellular ultrastructure is rapid to preserve cellular and vascular integrity (1).

Reversible injury induced by coronary artery occlusion for less than 20-30 min is reported to be indistinguishable from normal myocardium in equilibrium state (13, 14). Among the more potentially variable myocardial injuries produced by prolonged duration of coronary artery occlusion, differentiation of the reversible injury

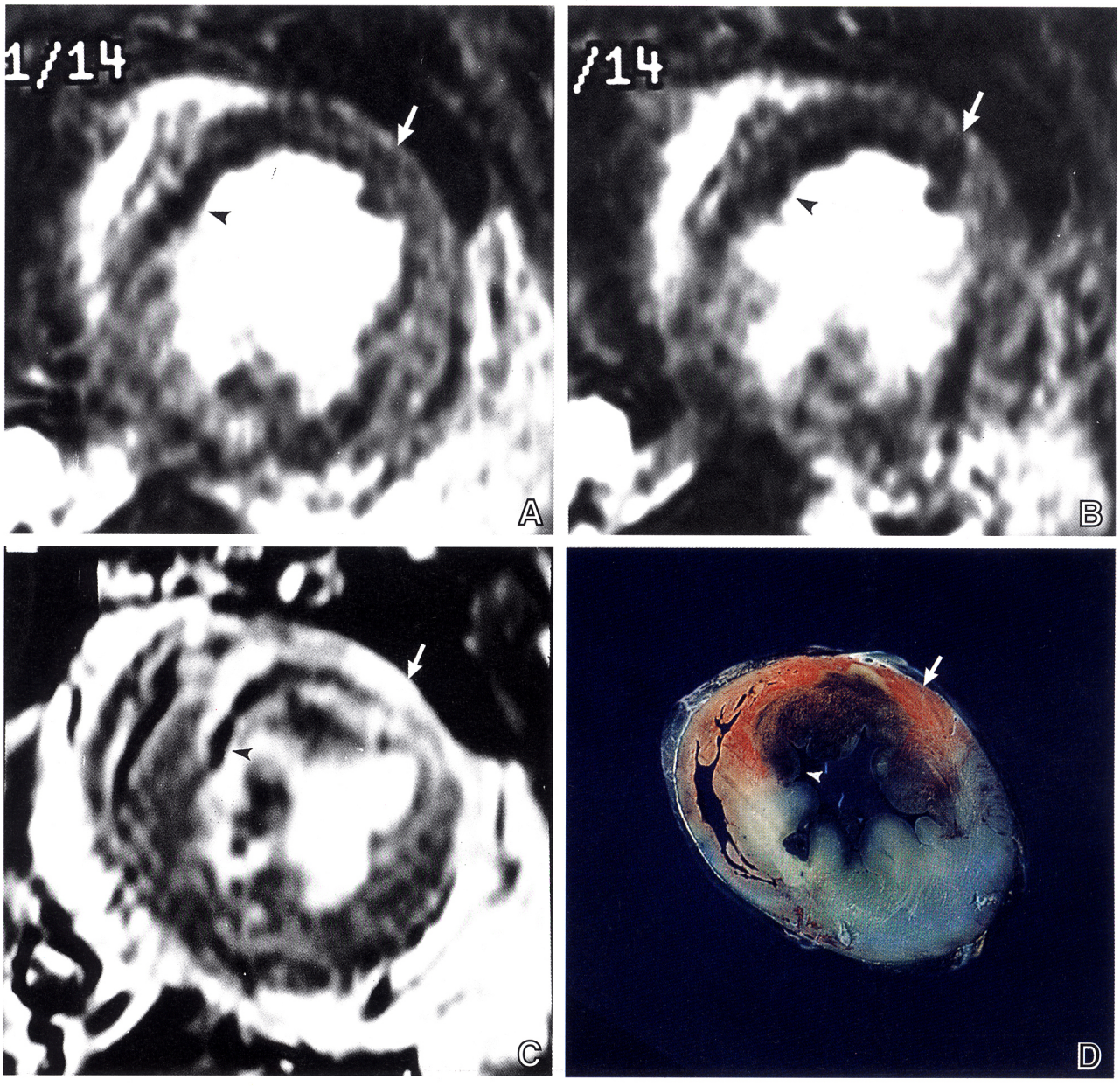

Fig. 2. Rest (A) and stress (B) first-pass FGRE images (post-contrast 14 sec), equivalent (C) steady-state SE image (post-contrast 5 min), and the TTC-stained specimen (D) of 3 hr occlusion and 30 min reperfusion model of a cat myocardium. Moderate subepicardial hypo-SI during stress (arrow, B) was the redistributed area during rest (arrow, A) in first-pass FGRE imaging and corresponds to peri-infarct zone in steady-state SE imaging (arrow, C). It is in agreement with brick-red colored rim of TTC-positive viable myocardium in stained specimen (arrow, D). The persistent subendocardial hypo-SI more accentuated during stress (arrowhead, B) in FGRE imaging corresponds to 'no-reflow' zone in SE imaging (arrowhead, C) and is corroborated by TTC-negative nonviable myocardium (arrowhead, D).

from either irreversible injury or normal myocardium has not been equally straight-forward. With the infarct size overestimation on contrast-enhanced MR images compared with histomorphometric analysis (15), some of the hyper-enhancing peri-infarct zone is attributed to the reversible injury (16, 17). First-pass MRI using IR-prepped echo-planar technique resulted in similar outcome as the reversible injury was indistinguishable from the normal myocardium while the occlusive or reperfused irreversible injury was shown as hypo- or delayed-enhancement, respectively (1). Therefore, the isolation of the reversible injury in MR imaging has been thus far not very promising. However, with the validation in identifying perfusion changes associated with coronary artery disease (18), first-pass MRI implemented with hyperemic agent may be potentially capable of differ-

entiating the reversible injury from the basally identifiable irreversible injury.

Previous studies using Gd-DTPA-labeled albumin associated hyper-enhancing peri-infarct zone with irreversible injury (13, 15, 19) which was confirmed histologically using biotin-labeled $(Gd\text{-}DTPA)_{30}$-albumin in combination with immunohistochemical staining (19). Enhancement of the peri-infarct zone has been attributed to extravasation of the compound due to the loss of microvascular integrity associated with myocytes necrosis (15). In the cases of compound such as Gd-DTPA-polylysine with molecular weight less than that of the albumin-labeled agent, association of peri-infarct zone has not been restricted to irreversible injury as such compound is less strictly confined to the vascular space (16, 17, 20). As such, outer peri-infarct zone in equilibrium state imaging of the current study was TTC-stained reversible injury consistent with the hypoperfused viable myocardium during stress which was redistributed at rest.

Gadomer-17 is a compound that satisfies the requirements of both perfusion and blood pool marker (20-23). Because of its large size, it is distributed in the intravascular space simplifying the transport kinetics which are governed mainly by flow and intravascular volume so that flow quantitation is possible (24). The high molecular weight (35 kDa) of the compound results in an increase in T1 relaxivity (17.3 L/mM/sec at 20 MHz) (21) which was observed in a phantom study comparing the compound with Gd-DTPA preliminary to the current study. While the shape of SI versus concentration profiles of the two compounds were similar, Gadomer-17 showed higher SI, approximately three times that of Gd-DTPA at lower concentration indicating the higher in vivo range of SI achievable by the compound. At delayed time, it remains largely confined within the intravascular space so that the plasma level is much higher than Gd-DTPA (24) causing adequately persistent blood pool and myocardial enhancement (16, 22). At the same time, the compound is small enough to be eliminated via the kidneys that its clearance from the body is reasonably rapid (20-23) preventing the deleteriously long blood pool enhancement seen in larger molecular weight compound which tends to inhibit clear delineation of the myocardial injury (25). It may provide a useful compromise between low molecular weight Gd-DTPA and the larger intravascular agents making it suitable for double bolus injections as in current study.

Various researches using contrast-enhanced MRI showed decreased perfusion secondary to complete coronary artery occlusion in animal models where simultaneously infused radioactive microspheres demonstrated that the distribution of contrast materials was proportional to flow. Rapid MR imaging was also applied in clinical environment to detect the differences between the normally perfused segments and segments supplied by diseased vessels. A delay in SI rise of the hypo-perfused myocardium permitted good correlation between segments identified as abnormal by MRI and by scintigraphy (19).

Areas of myocardium perfused by a diseased coronary artery have also been shown to have significantly reduced peak SI and a diminished up-slope of the intensity-versus-time curves (26). Pharmacologic stress test was proved effective in depicting the hypo-perfusion in partially occluded coronary arteries of canine heart (19, 20) where the normal myocardium demonstrated a greater enhancement relative to hypo-perfused myocardium after administration of dipyridamole than without the use of the vasodilator (18). Clinical study demonstrated up-slopes of greater variance among myocardial regions after stress than those of the curves obtained at rest, demonstrating the ability of dipyridamole stress in amplifying the flow differences among the regions (26). In the current study of feline reperfused infarction using short acting ATP as a stress agent, similar greater variance of myocardial perfusion was also displayed. This may be in accordance with the variable hyperemic response according to the microvascular integrity associated with the fraction of viable myocytes (27). The transmural perfusion gradient associated with the characteristic location and viability of the myocardial injuries was well displayed (Table 1, Fig. 2).

With the wash-in profile of the viable myocardium remaining relatively unchanged by the hyperemic stimuli, higher SI_{max} of the normal myocardium led to increased SI difference from the viable myocardium. Additional earlier occurrence of the SI_{max} of the normal myocardium also intensified the SI difference further as at this earlier time point, the SI reached by the viable myocardium is smaller (Fig. 1). This is consistent with the earlier occurrence of the larger Max ΔSI at hyperemic state. Therefore, in spite of the insignificant change in SI_{max}, the viable myocardium appeared altered as hypo-SI distinct from the surrounding more pronounced hyper-SI of the normal myocardium at this earlier time point of the Max ΔSI. Thus, with a small little time change leading to greater SI difference among the myocardial zones during the rapid 'washin' phase of the bolus transit, time of Max ΔSI may be crucial to the identification of the viable myocardium. This is evidenced by hyperemia induced significant change in Max ΔSI ($p=0.004$) but not in SI_{max} Ratio ($p=0.107$) for viable myocardium in Table 2 consistent with the inclusion of the time factor in the former but not the latter. With a hyperemic agent which results in greater left-ward shift of the bolus profile in the normal myocardium, more detailed identification of

the viable myocardium may be possible.

After the attainment of Max ⊿SI, subsequent rapid reduction in SI difference associated with the brisk downslope of the normal myocardium during the still ongoing 'washin' phase of viable myocardium may have led to the appearance of early redistribution in viable myocardium while such change was not noticeable in nonviable myocardium. Contrary to growing interest in using rest and stress regimen to identify viability within acute ischemic injury (27-31), identification of viable myocardium have not been complete previously. To validate the current finding of early redistribution in viable myocardium, further study may be valuable.

Histologic and electron microscopic studies in rats showed that irreversibly and reversibly damaged myocytes may reside next to each other in the same infarct territory and that each of these cells may vary with respect to degree and extent of alteration of its subcellular components (15). These changes depend on the duration of ischemia and are manifestated as differential blood volume and flow. Therefore, differential enhancement of myocardial regions in MRI may be more or less the consequence of differential fraction of irreversibly and reversibly damaged myocytes within the injury zones as reflected in the results of fluorescent microscopic examinations of the tissues (17). Consistent with this, reperfused reversible injury of predominant viable myocytes could not be differentiated from normal myocardium in previous observations (1, 13, 14).

Histologic examinations observed areas of hemorrhage with severely damaged ultrastructures within the infarct core (1, 16, 17) where the occluded vessel would lead to exclusion of the contrast agent during the first transit and absent response to the hyperemic stimuli as observed in nonviable myocardium of current study. On the other hand, moderately distorted ultrastructure at infarct periphery lead to release of items such as adenosine, various kinins, and histamin resulting in vasodilation (13, 16) so that the resting flow is not compromised but the response to the pharmacologic stimulation reduced (32, 33). With the uncompromised resting flow in viable myocardium contributing to its close approximation to the resting flow in normal myocardium, reduced hyperemic response leads to greater perfusion difference from the normal myocardium thereby leading to its identification.

In reperfused infarction, the combination of reduced myocardial high-energy phosphate stores, cell swelling, and sarcolemmal damage appears to play a key role in determining the viability outcome of the injured tissues (34). During the progression of infarction, the production of high-energy phophates declines and is greatly exceeded by their utilization leading to progressive depletion of phosphate stores within tissues. In reversible injury, such depletion is modest and electron microscopy may reveal only glycogen loss, nuclear chromatin aggregation, stretched myofibrils, and swollen mitochondria but no sarcolemmal damage (34, 35), endothelial nuclear chromatin clumping or margination (17). With further depletion leading to ATP content below 20 % of control values, cells become unable to regenerate high-energy phosphate or to maintain physiologic ionic gradients and cell volume. Consequent cell death in irreversible injury may reveal enlarged mitochondria with amorphous matrix densities, fractionation of myofilaments, sarcolemmal disruption (34, 35), endothelial swelling with protrusion, and decreased number of pinocytic vesicles (17).

With the myocardial infarction evolving to progressive increased fraction of nonviable myocytes (1, 16, 36-38), damage to microvascular endothelium, tissue swelling, and consequent reduction in blood volume and flow (10, 11) within myocardial injuries shown in rest and stress MRI were well reflective of the fractional composition of viable myocytes within the injury zones leading to the identification of the viable myocardium.

In conclusion, viable myocardium was identified in rest and stress MRI as redistributing hypo-perfusion distinct from persistent hyper-perfusion of the normal myocardium in addition to the persistent hypo-perfusion of the nonviable myocardium.

REFERENCES

1. Saeed M, Wendland MF, Yu KK, Lauerma K, Li HT, Derugin N, Cavagna FM, Higgins CB. *Identification of myocardial reperfusion with echo planar magnetic resonance imaging. Discrimination between occlusive and reperfused infarctions. Circulation 1994; 90: 1492-501.*
2. Higgins CB, Sakuma H. *Heart disease: functional evaluation with MR imaging. Radiology 1996; 199: 307-15.*
3. Edelman RR, Li W. *Contrast-enhanced echo-planar MR imaging of myocardial perfusion: preliminary study in humans. Radiology 1994; 190: 771-7.*
4. Wilke NM, Jerosche-Herold M, Zenovich A, Stillman AE. *Magnetic resonance first-pass myocardial perfusion imaging: clinical validation and future applications. J Magn Reson Imaging 1999; 10: 676-85.*
5. Sonoda S, Takeuchi M, Nakashima Y, Kuroiwa A. *Safety and optimal dose of intracoronary adenosine 5'-triphosphate for the measurement of coronary flow reserve. Am Heart J 1998; 135: 621-7.*
6. Shiode N, Kato M, Nakayama K, Shinohara K, Kurokawa J, Yamagata T, Matsuura H, Kajiyama G. *Effect of adenosine triphosphate on human coronary circulation. Intern Med 1998; 37: 818-25.*

7. Redberg RF, Sobol Y, Chou TM, Malloy M, Kumar S, Botvinick E, Kane J. *Adenosine-induced coronary vasodilation during transesophageal Doppler echocardiography. Rapid and safe measurement of coronary flow reserve ratio can predict significant left anterior descending coronary stenosis. Circulation 1995; 92: 190-6.*
8. Kato M, Shiode N, Teragawa H, Hirao H, Yamada T, Yamagata T, Matsuura H, Kajiyama G. *Adenosine 5'-triphosphate induced dilation of human coronary microvessels in vivo. Intern Med 1999; 38: 324-9.*
9. Kohno H, Yamada H, Azuma A, Kondo M, Yagi T, Kawata K, Tatsukawa H, Sugihara H, Nakagawa M. *Measurement of coronary flow reserve using adenosine 5'-triphosphate in dogs. J Cardiol 1998; 32: 1-8.*
10. Wendland MF, Saeed M, Lauerma K, Derugin N, Mintorovitch J, Cavagna FM, Higgins CB. *Alterations in T1 of normal and reperfused infarcted myocardium after Gd-BOPTA versus GD-DTPA on inversion recovery EPI. Magn Reson Med 1997; 37: 448-56.*
11. Lima JAC, Judd RM, Bazille A, Schulman P, Atalar E, Zerhouni EA. *Regional heterogeneity of human myocardial infarcts demonstrated by contrast-enhanced MRI: potential mechanisms. Circulation 1995; 92: 1117-25.*
12. Wu KC, Zerhouni EA, Judd RM, Lugo-Olivieri CH, Barouch LA, Schulman SP, Blumenthal RS, Lima JA. *Prognostic significance of microvascular obstruction by magnetic resonance imaging in patients with acute myocardial infarction. Circulation 1998; 97: 765-72.*
13. Wolfe CL, Moseley ME, Wikstrom MG, Sievers RE, Wendland MF, Dupon JW, Finkbeiner WE, Lipton MJ, Parmley WW, Brasch RC. *Assessment of myocardial salvage after ischemia and reperfusion using magnetic resonance imaging and spectroscopy. Circulation 1989; 80: 969-82.*
14. Schmiedl U, Sievers RE, Brasch RC, Wolfe CL, Chew WM, Ogan MD, Engeseth H, Lipton MJ, Moseley ME. *Acute myocardial ischemia and reperfusion: MR imaging with albumin-Gd-DTPA. Radiology 1989; 170: 351-6.*
15. Schwitter J, Saeed M, Wendland MF, Derugin N, Canet E, Brasch RC, Higgins CB. *Influence of severity of myocardial injury on distribution of macromolecules: extravascular versus intravascular gadolinium-based magnetic resonance contrast agents. J Am Coll Cardiol 1997; 30: 1086-94.*
16. Saeed M, Wendland MF, Masui T, Connolly AJ, Derugin N, Brasch RC, Higgins CB. *Myocardial infarction: assessment with an intravascular MR contrast medium. Work in progress. Radiology 1991; 180: 153-60.*
17. Lim TH, Lee JH, Gong G, Park SJ, Lee I. *Significance of magnetic resonance signal enhancement in evaluation of myocardial infarction in cats. Invest Radiol 1995; 30: 306-14.*
18. Saeed M, Wendland MF, Sakuma H, Geschwind JF, Derugin N, Cavagna FM, Higgins CB. *Coronary artery stenosis: detection with contrast-enhanced MR imaging in dogs. Radiology 1995; 196: 79-84.*
19. Saeed M, van Dijke CF, Mann JS, Wendland MF, Rosenau W, Higgins CB, Brasch RC. *Histologic confirmation of microvascular hyperpermeability to macromolecular MR contrast medium in reperfused myocardial infarction. J Magn Reson Imaging 1998; 8: 561-7.*
20. Schuhmann-Giampieri G, Schmitt-Willich H, Frenzel T, Press WR, Weinmann HJ. *In vivo and in vitro evaluation of Gd-DTPA-polylysine as a macromolecular contrast agent for magnetic resonance imaging. Invest Radiol 1991; 26: 969-74.*
21. Clarke SE, Weinmann HJ, Lucas A, Dai E, Rutt BK. *MR angiography at 0.5T with Gadomer-17, a new blood pool agent: dose study and comparison with 2D TOF in rabbits (abstract). In: Proceedings of the International Society for Magnetic Resonance in Medicine 1998. Sydney: International Society for Magnetic Resonance in Medicine, 1998; 215.*
22. Lim TH, Lee DH, Kim YH, Park SW, Park PH, Seo DM, Kim ST, Lee TK, Mun CW. *Occlusive and reperfused myocardial infarction: detection by using MR imaging with gadolinium polylysine enhancement. Radiology 1993; 189: 765-8.*
23. Wang Z, Redpath JL, Su MY, Lao X, Nalcioglu O. *Radiation induced tumor vascular permeability and the effective interstitial space volume changes as measured by the dynamic Gadomer-17 enhanced MRI [abstract]. In: Proceedings of the International Society for Magnetic Resonance in Medicine 1998. Sydney: International Society for Magnetic Resonance in Medicine, 1998; 60.*
24. Wilke N, Kroll K, Merkle H, Wang Y, Ishibashi Y, Xu Y, Zhang J, Jerosch-Herold M, Mühler A, Stillman AE, Bassingthwaighte JB, Bache R, Ugurbil K. *Regional myocardial blood volume and flow: first-pass MR imaging with polylysine-Gd-DTPA. J Magn Reson Imaging 1995; 5: 227-37.*
25. Roberts HC, Saeed M, Roberts TP, Mühler A, Shames DM, Mann JS, Stiskal M, Demsar F, Brasch RC. *Comparison of albumin-$(Gd\text{-}DTPA)_{30}$ and Gd-DTPA-24-cascade-polymer for measurements of normal and abnormal microvascular permeability. J Magn Reson Imaging 1997; 7: 331-8.*
26. Eichenberger AC, Schuiki E, Kochli VD, Amann FW, McKinnon GC, von Schulthess GK. *Ischemic heart disease: assessment with gadolinium-enhanced ultrafast MR imaging and dipyridamole stress. J Magn Reson Imaging 1994; 4: 425-31.*
27. Iliceto S, Galiuto L, Marchese A, Cavallari D, Colonna P, Biasco G, Rizzon P. *Analysis of microvascular integrity, contractile reserve, and myocardial viability after acute myocardial infarction by dobutamine echocardiography and myocardial contrast echocardiography. Am J Cardiol 1996; 77: 441-5.*
28. Cherryman GR, Hudson N, Moody AR, Jivan A, Early M, Woods K. *Dynamic perfusion imaging in patients with acute myocardial infarction: comparison with TI-201 SPECT. 82nd assembly and annual meeting of the Radiological Society of North America 1996. Radiology 1996; 201(Suppl): 165.*
29. Muller S. *MR tomography studies of myocardial function and perfusion after myocardial infarction. Rofo. Fortschriftte auf dem Gebiete der Roentrenstrahlen und der Neuen Buildgeben-*

den Verfahren 1997; 167: 339-405.

30. Wilke N, Jerosch-Herold M, Wang Y, Huang Y, Christensen BV, Stillman AE, Ugurbil K, McDonald K, Wilson RF. *Myocardial perfusion reserve: assessment with multisection, quantitative, first-pass MR imaging. Radiology 1997; 204: 373-84.*
31. Lepper W, Hoffmann R, Kamp O, Franke A, de Cock CC, Kühl HP, Sieswerda GT, Dahl JV, Janssens U, Voci P, Visser CA, Hanrath P. *Assessment of myocardial reperfusion by intravenous myocardial contrast echocardiography and coronary flow reserve after primary percutaneous transluminal coronary angiography in patients with acute myocardial infarction. Circulation 2000; 101: 2368-74.*
32. Davis CP, Liu PF, Hauser M, Göhde SC, von Schulthess GK, Debatin JF. *Coronary flow and coronary flow reserve measurements in human with breath-hold magnetic resonance phase contrast velocity mapping. Magn Reson Med 1997; 37: 537-44.*
33. Pennel DJ, Underwood SR, Ell PJ, Swanton RH, Walker JM, Longmore DB. *Dipyridamole magnetic resonance imaging: a comparison with thallium-201 emission tomography. Br Heart J 1990; 64: 362-9.*
34. Ganz P, Braunwald E. *Coronary blood flow and myocardial ischemia. In: Braunwald E, editor. Heart Disease, 5th ed. Philadelphia: W.B. Saunders, 1997; 1161-83.*
35. Jennings RB, Schaper J, Hill ML, Steenbergen C, Reimer KA. *Effect of reperfusion late in the phase of reversible ischemic injury: changes in cell volume, electrolytes, metabolites, and ultrastructure. Circ Res 1985; 56: 262-78.*
36. Wendland MF, Saeed M, Canet E, Higgins CB. *Potential measurement of viable cell fraction in reperfused myocardial infarction using Gd-enhanced IR-EPI [abstract]. In: Proceedings of the International Society for Magnetic Resonance in Medicine 1997. Vancouver: International Society for Magnetic Resonance in Medicine, 1997; 846.*
37. Klein MA, Collier BD, Hellman RS, Bamrah VS. *Detection of chronic coronary artery disease: value of pharmacologically stressed, dynamically enhanced Turbo-Fast Low-Angle Shot MR images. Am J Roentgenol 1993; 161: 257-63.*
38. Borges-Neto S, Watson JE, Miller MJ. *Tc-99m sestamibi cardiac SPECT imaging during coronary artery occlusion in humans: comparison with dipyridamole stress studies. Radiology 1996; 198: 751-4.*